Multi-Voxel Pattern Analysis of Human Emotion and Memory Guided by Neurosynth

Jiachuan Wang

Bachelor of Science

College of Medicine and Veterinary Medicine

University of Edinburgh

2023

Acknowledgement

The author thanks the supervisor, Dr. Gediminas Lukšys for his scientific input, helpful comments, and generous support.

Abstract

Describing the neural architecture behind episodic memory encoding and the processes involved in the memory enhancement effect is at the heart of memory neuroscience. Functional magnetic resonance imaging as a real-time recording and non-invasive technology has revolutionized the paradigm of brain science research, providing the possibility of in-depth study of the neural basis of memory and emotional processes. Unlike the univariate approaches used in past neuroimaging studies, multi-voxel pattern analysis not only captures the joint activity of distributed neural ensembles that support cognitive functions, but also considers the possibility that insignificant voxels encode responses. I conducted brain mapping and multi-voxel pattern analysis on the emotional dimensions and memory retrieval performance in the picture task through brain region information from real data and the meta-analysis database Neuorsynth. The results reveal the neural basis of emotion and memory-related phenotypes distributed in cortical areas and the bias toward subcortical components of the limbic system in previous studies, which has a cautionary implication on regions of interest selection in neuroimaging research.

Keywords: functional neuroimaging, multi-voxel pattern analysis, limbic system, episodic memory, recognition memory

Table of contents

List of figures and tables

List of abbreviations

AG	Angular Gyrus
ANN	Artificial Neural Network
ANOVA	Analysis of Variance
ARAS	Ascending Reticular Activation System
Cu	Cuneus
EEG	Electroencephalography
fMRI	Functional Magnetic Resonance Imaging
FPR	False Positive Rate
FuG	Fusiform Gyrus
FWER	Family-wise Error Rate
GLM	General Linear Model
HRF	Hemodynamic response function
IAPS	International Affective Picture System
IC	Independent Component

ICA	Independent Component Analysis
IOG	Inferior Occipital Gyrus
LG	Lingual Gyrus
MD	Difference in Means
MEG	Magnetoencephalography
MNI	Montreal Neurological Institute
MOG	Middle Occipital Gyrus
MVPA	Multi-voxel Pattern Analysis
PET	Positron Emission Tomography
PoCG	Postcentral Gyrus
PrCG	Precentral Gyrus
PrCu	Pre-cuneus
RBF	Radial Basis Function
RG	Rectus Gyrus
ROI	Region of Interest
SFG	Superior Frontal Gyrus
ss-EPI	Single-shot Echo-planar Imaging
SVC	Small-volume Correction
SVM	Support Vector Machine

Introduction

Outline of brain mapping

Brain mapping is a neuroscience topic that aims to associate cognition and behavior with the brain structure. It typically involves the application of various neuroimaging techniques, including functional magnetic resonance imaging (fMRI), electroencephalography (EEG), positron emission tomography (PET), and magnetoencephalography (MEG) (Siddiqi *et al.*, 2022).

An early example of brain mapping was Paul Broca's discovery that damage to a specific area of the left frontal lobe in the human brain would lead to language impairment (Broca, 1861; Dronkers *et al.*, 2007). Over time, other lesion studies were performed to project brain regions onto various functions such as motor control and sensory processing (Baier *et al.*, 2009; Muckli *et al.*, 2009). In the 20th century, new technologies such as fMRI and PET were developed, which allow researchers to map brain function in real time (Fox *et al.*, 1986; Ogawa *et al.*, 1992). These advances in noninvasive imaging have led to breakthroughs in understanding how the brain works, including discovering the brain's default mode network (Greicius *et al.*, 2003).

Nowadays, brain mapping is an essential set of tools in neuroscience research and clinical practice. It has been used not only to diagnose diseases such as epilepsy, Parkinson's disease, and stroke but also to understand the neural basis of cognitive processes such as attention, emotion, and memory (Callicott *et al.*, 1998; Nour and Liebeskind, 2011; Doucet *et al.*, 2014; Dubois *et al.*, 2020; Vignando *et al.*, 2022; Zhao *et al.*, 2022). By identifying brain regions involved in specific processes, we can better understand how the brain supports behavior, which may help develop new treatments for neurological and psychiatric disorders through new insights into cognitive impairment and conditions that affect brain function. Brain mapping can also provide insights into the mechanisms underlying human cognition, which can help advance our understanding of the brain and human existence more broadly.

Research in episodic memory and emotion

As an essential part of human cognition, memory is a prerequisite for developing language and personal identity (Eysenck, 2012). The ‘memory’ in common sense usually refers to explicit memory in scientific terms, which consists of episodic and semantic memory (Tulving, 2002). Furthermore, episodic memory refers to the recollection of daily events that can be declared, including contextual and subjective information such as time, place, and emotion (Schacter *et al.*, 2009).

Research on episodic memory has been ongoing for decades and has made significant contributions to our understanding of the nature and function of this type of memory. Studies have shown that the hippocampus and associated structures are critical in episodic memory encoding and consolidation (Fernandes *et al.*, 2005; Schacter, 2008). In addition, a widely accepted idea is that specific types of memories are stored long-term in specific cortical regions (Frankland and Bontempi, 2005). Researchers also examined the cognitive processes involved in retrieving episodic memories, including emotion regulation. Emotions can be represented using two dimensions of valence and arousal, with high arousal and positive/negative valence contributing to successful recall (Fig. 1; Russell, 1980; Kensinger E.A., 2004; Kragel and LaBar, 2016). The amygdala, the center of emotional control in the human brain, is thought to be involved in memory enhancement (Cahill *et al.*, 1995; Calder *et al.*, 2001).

Past research has linked the limbic system, including subcortical components such as the hippocampus and amygdala, to emotional and memory processes (Morgane *et al.*, 2005). Recently, more and more studies suggest that cognitive functions result from the interaction of various distributed neural representations in cortical and subcortical regions (Rissman and Wagner, 2012; Kragel and LaBar, 2016). Research on episodic memory has helped to shed light on the fundamental processes involved in memory acquisition and retrieval, which has important implications for understanding a wide range of cognitive functions and psychological disorders like amnesia (Rajah and D'Esposito, 2005).

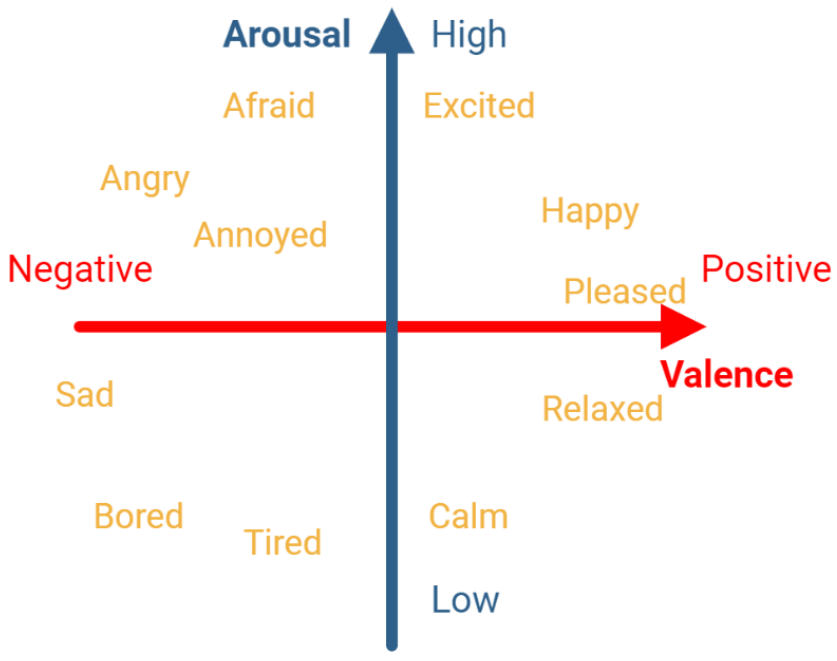

Figure 1. Dimensional model in emotions field.

Coordinates of some example emotions, defined by valence and arousal.

Given the noninvasive nature, fMRI has been used extensively to study the neural mechanisms that underlie episodic memory and emotion, including mapping different stages of memory onto brain regions, for example, encoding and retrieval stages (Rajah and D'Esposito, 2005; Dubois *et al.*, 2020). However, the retrieval process can be differentiated into free recall and recognition according to uncued or cued recall. Few studies have examined neural representations of different retrieval processes, which may overlook specific memory mechanisms.

fMRI data analysis pipeline and multi-voxel pattern analysis

The most basic fMRI data analysis steps include preprocessing, first-level and second-level analyses (Worsley *et al.*, 2002). The preprocessing of the raw data involves operations such as correction of head motion, breathing, heartbeat, and other noises (Hutton *et al.*, 2011). In addition, to ensure that brain images from different trials are comparable, they would be aligned into the same space. The Montreal Neurological Institute (MNI) space/template is commonly used (Evans *et al.*, 1993). The first-level model fits the response predicted by convolution of the hemodynamic response function (HRF) with the experimental stimulus paradigm to the time-series data at each voxel (a small unit divided on a regular grid of 3D space) (Aguirre *et al.*, 1998). For group-level analyses, second-level analyses utilize statistical tests such as *t*-tests to make broader inferences about brain activity (Friston *et al.*, 1999).

Given the large number of voxels with multiple comparisons, the false positive rate would inflate, so setting a correction threshold is crucial (Chumbley and Friston, 2009). Some researchers use small-volume correction (SVC) to threshold the activation maps based on the voxels in the region of interest (ROI) (Poldrack, 2007). Contrary to conservative whole-brain analyses, ROI-based correction tends to result in a more loose threshold that may suggest meaningful results but may also exaggerate the contribution of some brain regions (Kriegeskorte *et al.*, 2009).

In neuroimaging studies, the selection of ROIs is often based on prior knowledge from the literature. Unregistered ROIs may be ambiguous in anatomical space, leading to inflated estimates of ROIs cited in later studies (Hong *et al.*, 2019). Large-scale meta-analyses of literature may provide precise definitions of ROIs (Lettieri *et al.*, 2019). An example is the data mining and brain mapping database Neurosynth, which reports the association of specific terms (e.g., 'valence', 'memory retrieval', and ''recognition') with voxel activations in published fMRI studies (Yarkoni *et al.*, 2011). The association maps generated via machine learning have the potential to provide a reference for ROI selection in subsequent studies.

Unlike second-level analyses that use single voxels or averaged brain region activity to predict

cognitive content, multi-voxel pattern analysis (MVPA) reduces neural responses into activation patterns, allowing researchers to investigate whether the brain regions used for decoding reveal information about specific cognitive states (Poldrack, 2011; Haxby, 2012). For MVPA, a commonly used decoding model is the support vector machine (SVM) with radial basis function (RBF) kernel (Ben-Hur *et al.*, 2008; Mahmoudi *et al.*, 2012). SVMs are advantageous for dealing with high-dimensional data and can represent the distributional hypothesis of neural activity in many cognitive processes like episodic memory encoding and storage, thus outperforming the general linear model (GLM) (Ben-Hur *et al.*, 2008; Mahmoudi *et al.*, 2012; Kriegeskorte and Douglas, 2019).

Aims

Because few studies in the fMRI field have used single-trial signals and focused on activity patterns under free recall and recognition tasks, I aim to perform brain mapping of different memory retrieval processes and use MVPA to predict the cognitive states on a single-trial basis of fMRI signals.

I would analyze the fMRI activity patterns of individual subjects in response to picture stimuli in an encoding task, projecting (1) free recall performance, (2) recognition performance, (3) emotional valence, and (4) arousal to brain regions, and performing decoding tasks. First, I hypothesize that brain regions responsible for emotions and memory are dispersed across the anatomical cortical areas. Second, I hypothesize that the numerous published fMRI studies are biased towards subcortical regions in the limbic system, such as the hippocampus and amygdala, which would negatively impact emotion and memory decoding. Third, I expect to compare the performance of multiple MVPA methods to achieve the highest possible accuracy in emotion and memory prediction.

Materials and methods

To avoid disclosure of personal information by online hosting services, scripts are available upon request.

Picture task description

The behavioral task was devised and administered by faculty members at the Department of Psychology, University of Basel, where 992 healthy Swiss adults conducted picture encoding and rating, free recall, and recognition tasks (Fig. 2, Luksys *et al.*, 2015).

First, the subjects were shown 72 pictures selected from the International Affective Picture System (IAPS) inside the scanner (Bradley and Lang, 2007). During each trial, the visual stimulation followed an event-related design, consisting of a fixed cross and an IAPS picture (Fig. 2a). After being shown the picture, the subjects rated emotional valence and arousal by pressing a button. Rating options include positive, neutral, and negative for valence and low, medium, and high for arousal.

Then subjects conducted an unannounced free picture recall task outside the scanner, writing brief comments about pictures they had seen in the previous encoding task. Two investigators independently assessed whether participants successfully recalled each picture, rating it as remembered or not-remembered. No time limit was set for this task.

After completing the free recall task, the subjects returned to the scanner for a 20-minute picture recognition task. Each trial consisted of a cross and a picture, similar to the paradigm in the encoding task (Fig. 2b). The pictures displayed contain those previously shown in the encoding task, also brand-new ones. Subjects were required to rate them as remembered, familiar, or new.

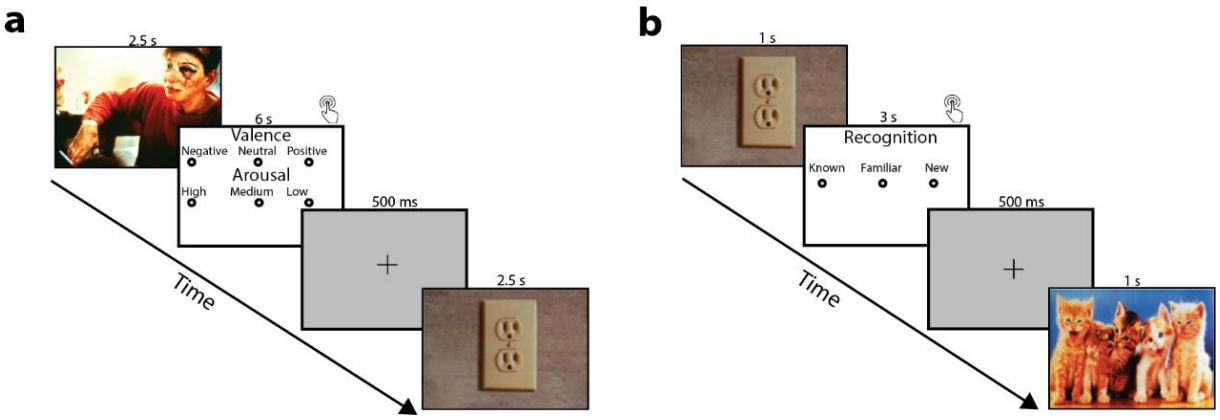

Figure 2. Paradigms of the picture task (Pater *et al.*, 2018)**.**

Figure 2. Paradigms of the picture task (Pater *et al*., 2018)**.**

(a) Picture encoding and rating task. A cross was displayed for 0.5 s on the video goggles, preceded by a 2.5 s picture presentation. Subjects then pressed their finger on the button within 6 s and rated each picture on their subjective emotional valence and arousal. **(b)** Picture recognition task. In each trial, a cross was displayed for 0.5 s, followed by a 1 s picture presentation, which may or may not have appeared during the encoding task. Within up to 3 s after each picture was presented, subjects pressed a button to rate on a three-point scale of remembered, familiar, and new.

fMRI data acquisition, preprocessing, and first-level analysis

The fMRI data were collected for preprocessing and first-level analysis by the faculty members of the Department of Psychology, University of Basel. The functional images were obtained with single-shot echo-planar imaging (ss-EPI) using a Siemens MAGNETOM Verio 3-T whole-body MR unit and a 12-channel head coil. Voxel size was set to 2.75 × 2.75 × 4 mm^3. The image data acquisition parameters and the description of correction, alignment, normalization, and smoothing steps are detailed in the paper of Luksys *et al*. (2015). Functional images were mapped to MNI space.

The first-level analysis within a single trial estimated the per-voxel contrast values (regression coefficient β) using a GLM convolving the visual stimulus and the canonical hemodynamic response function (HRF). SPM8 software was used to run the first-level model and the above preprocessing operations (Penny *et al.*, 2007; Poldrack *et al.*, 2011). The resulting brain volume dimension was 67 × 46 × 80. Subsequent group analysis used a subset containing information on 100 subjects.

fMRI second-level analysis

The second-level analysis was implemented in Python 3.9. The fixed effects model was adapted to test the difference between groups on the β vectors voxel-by-voxel. The *t*-statistics were obtained by comparing two samples, which included different valence (positive vs. neutral, negative vs. neutral), arousal (high vs. low), free recall performance (remembered vs. not-remembered), and recognition performance (old vs. familiar-new, because of few records in the latter two categories) conditions. The *T* map generated by the model was normalized by the following formula, converting into a *Z* map:

$$Z = \frac{X - \mu}{\sigma}$$

Equation 1

where:

μ is the population mean,

σ is the standard deviation of the population.

The voxel-wise significance level was first accepted at 0.001 (corresponding to absolute $Z > 3.2905$). Family-wise error rate (FWER) of 0.05 controlled by the Bonferroni procedure was tried to perform the multiple comparison correction at the whole-brain level.

The following affine array was applied to the voxel coordinates to map to the MNI system.

$$\begin{bmatrix} -2.75 & 0. & 0. & 90.75 \\ 0. & 2.75 & 0. & -126.5 \\ 0. & 0. & 4. & -72. \\ 0.0 & 0. & 0. & 1. \end{bmatrix}$$

Neurosynth maps preprocessing and comparison

As a reference for voxels associated with cognitive status, association test maps synthesized by meta-analysis were downloaded from the online database Neurosynth (version 0.7, last updated in July 2018). The shape of the Neurosynth maps is 91 × 109 × 91, with a single voxel size of 2 × 2 × 2 mm^3. Neurosynth maps were resampled on the Basel data as the target via the resample_to_img function in the Nilearn package. A selection of terms that may be relevant to the cognitive state of the picture task is listed in Table 1. When visualizing Neurosynth maps, FWER was set to 0.05.

Valence		Arousal	Free recall	Recognition
Positive vs. neutral	Negative vs. neutral			
Emotional valence	Emotional valence	Arousal	Recall	Recognition memory
Valence	Valence		Episodic memory	Recognition
Happy	Unpleasant		Memory retrieval	Episodic memory
Pleasant	Negative emotions		Subsequent memory	Memory retrieval
				Subsequent memory

Table 1. Candidate Neurosynth terms for each prediction domain.

Table 1. Candidate Neurosynth terms for each prediction domain.

Terms picked from the Neurosynth database that were thought to be relevant to the picture task. Note that there are no terms such as positive emotions, wakefulness, and free recall in Neurosynth.

The data comparison used the top hits in the Basel data second-level analysis results and the corresponding voxels in the Neurosynth maps rather than the whole brain voxels. The top hits are voxels with uncorrected *p*-value < 0.001. The Pearson correlation coefficient (Pearson's *r*) was calculated using the Z-score vectors of each pair of the two maps, then corresponded to the two-sided *p*-value (Student, 1908).

Point-to-point Z-score comparisons were performed by selecting representative voxels in brain regions with the most significant activity/association in Basel data and Neurosynth maps. Brain region information was extracted based on the JHU_MNI_SS_BPM_TypeII_ver2.1 atlas (Faria ***et al.***, 2012).

MVPA

In this experiment, the dimensionality reduction techniques include ‘top-voxel’, Neurosynth-guided, and ICA-based approaches, applying to the β-vectors of every single trial. Binary-classifier-based MVPA was built and trained, aiming to predict valence, arousal, free recall performance, and recognition performance on a single trial basis. Given some incomplete ratings in the encoding and recognition tasks, the corresponding β records were omitted, with sample sizes reported in the results section. All analyzes were run in Python 3.9.

Feature selection

For model simplification and to avoid overfitting, 100 features were used as input to the classifier. The ‘top-voxel’ approach was based on the Z map given by the second-level analysis. To include informative voxels from more diverse brain regions, this approach iteratively applies an exclusion of 2-voxel radius to each selected voxel based on selecting the voxel with the highest absolute Z-score, that is, the surrounding 26 voxels of an already selected one would not be selected in one prediction task. The Neurosynth-guided approach uses the resampled Neurosynth map and selects the 100 voxels with the highest absolute Z-score. The independent component analysis (ICA)-based approach was based on the Fast ICA algorithm of scikit-learn 1.2.2, which is fitted to all trials under the condition to be predicted. The first 100 independent components (ICs) were used as

input variables for subsequent classifications.

Classifier architecture, training, evaluation, and optimization

The features were first standardized according to Equation 1. The L2 regularized logistic regression (C = 1) implemented in scikit-learn 1.2.2 was used as the benchmark model with the default parameters. The SVM inherited the SVC function with the RBF kernel, which is given by:

$$K\ (x, x') = exp(-\gamma \|x - x'\|^2)$$

Permutation tests were performed by randomly shuffling the labels during model training to obtain the chance level of prediction, with SVM controlled by default parameters. Classification metrics reporting precision, recall, F1-score (weighted harmonic mean of precision and recall), and support (size of the test set) for each class were output. The reported averages include the macro and weighted ones, calculated by averaging the unweighted or support-weighted mean per label.

$$precision\ = \frac{TP}{TP + FP}$$

$$recall\ = \frac{TP}{TP + FN}$$

where,

TP refers to the number of true positives,

FP refers to the number of false positives,

FN refers to the number of false negatives.

The fine-tuning of SVMs was done by changing the value of the hyperparameter γ and regularization constant C via Grid search (Table 2). Model training and testing utilized 5-fold cross-validation. When comparing model accuracy under different feature selection techniques, four replicates of 5-fold cross-validations were run.

Statistics and visualization

The statistical methods used in the second-level analysis were described in the corresponding section. Inter-group comparisons of model accuracies were performed by two-way or three-way Analysis of Variance (ANOVA) with Tukey's test or the semi-parametric alternative ordinal cumulative probability model with Šidák correction (Harrell, 2015). Diagnostic plots were examined as evidence

of the normality of residuals and homoscedasticity. Visualization of brain images was made using Nilearn. Statistical graphs were plotted using R version 4.0.4.

Prediction tasks		Feature selection techniques	Parameter settings (log increment)	
			γ	C
Valence	Positive vs. neutral	'top-voxel'	1×10^{-9} – 1×10^{-3} (0.6)	10 – 1×10^{5} (0.4)
		Neurosynth-guided	1×10^{-7}, 1×10^{-5}, 1×10^{-3}, 1	1×10^{-6} – 1 (2)
		ICA-based	1×10^{-5} – 0.1 (0.4)	0.01 – 1×10^{4} (0.6)
	Negative vs. neutral	'top-voxel'	0.32 – 1×10^{5} (0.55)	1×10^{-5} – 0.001 (0.3)
		Neurosynth-guided	1×10^{-5} – 100 (1)	0.1 – 100 (1)
		ICA-based	1×10^{-4} – 1×10^{-2} (0.2)	0.32 – 100 (0.25)
Arousal	High vs. low	'top-voxel'	1×10^{-4} – 0.1 (0.2)	0.32 – 31.62 (0.13)
		Neurosynth-guided	1×10^{-4} – 3.16×10^{-3} (0.5)	0.03 – 3.16 (0.5)
		ICA-based	1×10^{-5} – 0.1 (0.4)	0.1 – 1×10^{4} (0.5)
Free recall	Remembered vs. not-remembered	'top-voxel'	0.0001 – 1 (0.5)	0.1 – 1×10^{4} (0.25)
		Neurosynth-guided	0.1	10
		ICA-based	0.1 – 0.0001 (0.1)	0.01 – 10 (0.15)
Recognition	Old vs. familiar-new	'top-voxel'	1.78×10^{-3} – 0.1 (0.0875)	0.01 – 1000 (0.4)
		Neurosynth-guided	1×10^{-3}	1×10^{-4}
		ICA-based	1×10^{-3} – 0.1 (0.1)	0.1 – 17.78 (0.1125)

Table 2. Bias-variance scheme.

The increments used common logarithmic increments. E.g., 0.1 – 1000 (2) means 0.1, 10, 1000. The reason for the various parameter ranges between feature selection techniques and phenotypes is that the optimal parameters for a model depend on the specific objective and the characteristics of the data.

Results

Potential neural representative of cognitive states of emotion and memory

I performed second-level analyses of the fMRI data in the picture encoding task, extracting *t*-statistics for each voxel in response to each condition pair (see Methods section). No voxels survived after Bonferroni correction (FWER < 0.05). Observations of voxels with uncorrected *p*-values < 0.001 showed that the informative patterns were mainly distributed in focused clusters in various cortical areas, especially in the occipital lobe, because of the visual-related nature of the behavioral tasks (Fig. 3).

When stimulated by pictures with subjectively positive valence, a larger cluster in the right middle occipital gyrus (MOG) and a small one in the left cuneus (Cu) were activated, while the left inferior occipital gyrus (IOG) was deactivated (Fig. 3a). Negative valence was correlated with modest left IOG activation (Fig. 3b). Pictures with higher arousal showed a weaker correlation with activation in right lingual gyrus (LG) (Fig. 3c). Successful free recall for pictures was related to activity in multiple cortical areas: a widespread activation in the left LG, and clusters in the left Cu, right MOG, fusiform gyrus (FuG) spanning the left temporal and occipital lobes (Fig. 3d). In addition to the deactivation in the left cerebellum, picture recognition memory exhibited a high degree of left hemisphere lateralization: inhibitory activity of the FuG, pre-cuneus (PrCu), LG, angular gyrus (AG), and the activation in the precentral gyrus (PrCG) (Fig. 3e).

Among these top hits, no significant voxels were found in the hippocampus or amygdala, which are thought to play important roles in memory and emotional processing.

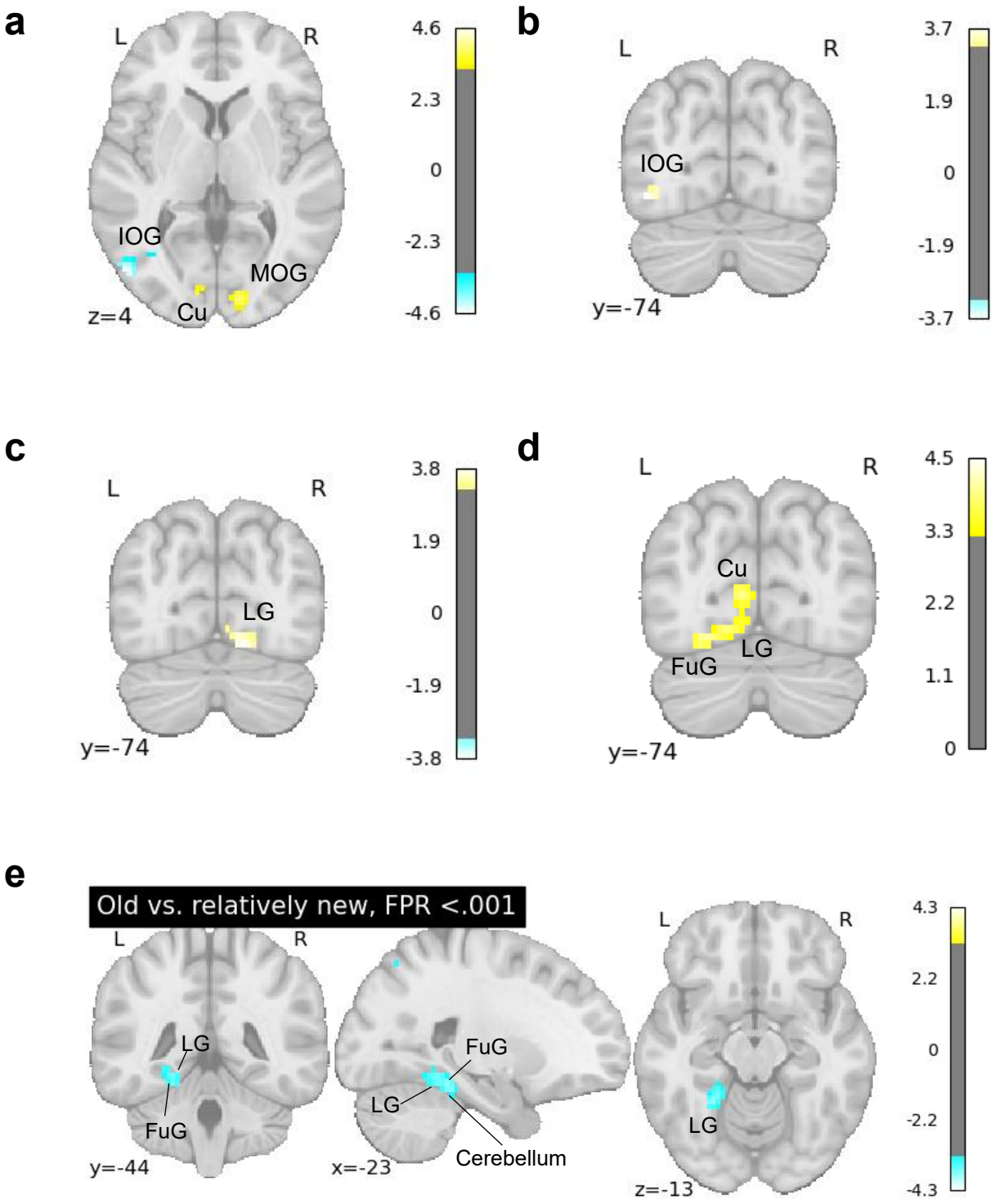

Figure 3. Activation maps under conditions of emotion and memory performance.

Differences in brain activity between **(a)** positive vs. neutral valence, centered at (-50, -72, 4) (n = 4,980), **(b)** negative vs. neutral valence, centered at (-41, -74, -7) (n = 4,736), **(c)** high vs. low arousal, centered at (12, -74, -7) (n = 4,272), **(d)** remembered vs. not-remembered in free recall, centered at (-15, -74, -9) (n = 7,200), and **(e)** old vs. relatively new (familiar and new) in recognition memory, centered at (-23, -44, -13) (n = 7,084). Threshold: absolute Z > 3.2905 (equivalent to uncorrected p < 0.001). FPR, false positive rate. MOG, middle occipital gyrus. Cu, cuneus. IOG, inferior occipital gyrus. LG, lingual gyrus. FuG, fusiform gyrus.

Mismatches in brain region activity patterns between Basel data and Neurosynth maps

I compared the second-level analysis results of the real data from Basel with the meta-analysis results from Neurosynth, to investigate their differences in the patterns of brain activity. First, I browsed the candidate terms (see Table 1) related to emotional valence and arousal, and memory, which may contain information related to cognitive state and behavioral tasks as a guide for MVPA. Because of the discrete distribution of brain representations of emotion and memory, I extracted limited significant voxels ($p < 0.001$) in activation maps of Basel data to test the correlation. Using the top hits in Basel data, I performed correlation analysis with the Z-scores of corresponding voxels in Neurosynth maps. The obtained Pearson's *r* value showed that the correlations between the activity of the brain regions in Basel data and Neurosynth maps are very low, even presenting a lot of negative correlations (Table 3).

I screened out the top hits of Neurosynth maps, with an FWER thresholded to 0.05. Almost all amygdala voxels were significant in association maps of the emotion-related terms, and many of the voxels located in the hippocampus were also significant in the memory-related maps (Fig. 4a). These top hits do not overlap with the Basel data ones with $p < 0.001$. So, I took individual voxels and performed point-to-point comparisons. By contrasting high versus low arousal, the peak voxel of the right amygdala held the highest Z-score of the whole brain in the arousal term, but it was not significant in the Basel data and dramatically lower than many other voxels (Fig. 4a & 4b). LG in the cortical area with a suggested correlation with arousal can have a higher rank in the Neurosynth map, whereas the low absolute value of its Z-score showed non-significance (Fig. 4c).

In summary, Neurosynth's modeling results based on bulk published studies and the results from our human emotion and memory research were critically mismatched. However, to study the predictive capability of Neurosynth maps, I selected the terms with the highest *r* values under each experimental condition pair, except for recall, because the *r* values of the candidate terms for free recall were not greater than 0.05, and the recall term is more intuitively related to the task.

	r	*p*	n
Positive vs. neutral valence			
Emotional valence	0.11	0.38	53
Valence	-0.10	0.41	
Happy	0.13	0.30	
Pleasant	0.09	0.47	
Negative vs. neutral valence			
Emotional valence	-0.06	0.81	11
Valence	0.06	0.82	
Unpleasant	-0.02	0.94	
Negative emotions	0.03	0.91	
High vs. low arousal			
Arousal	0.05	0.79	28
Free recall			
Recall	0.02	0.72	209
Episodic memory	-0.01	0.84	
Memory retrieval	0.03	0.64	
Subsequent memory	0.05	0.51	
Recognition			
Recognition memory	-0.01	0.88	92
Recognition	0.05	0.60	
Episodic memory	-0.30	0.00	
Memory retrieval	-0.25	0.01	
Subsequent memory	-0.02	0.85	

Table 3. Correlation results for different Neurosynth terms.

Pearson's *r*, *p*-value, and number of samples between the Z-scores of Basel data and Neurosynth map (only comparing the voxel with $p < 0.001$ in Basel data). Blue denotes the terms selected for subsequent MVPA guidance.

a

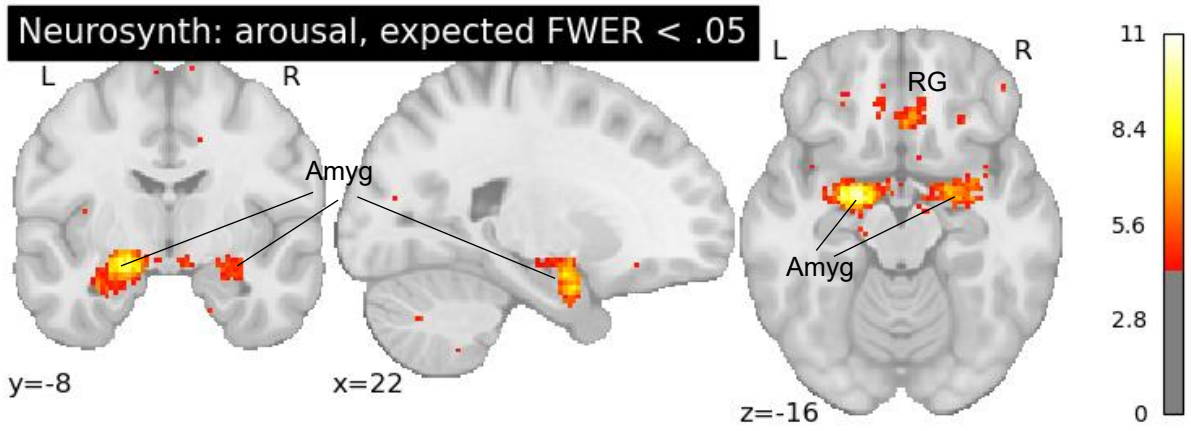

b

MNI coordinate			Z-score (percentile)		Brain region
x	y	z	Basel	Neurosynth	Right amygdala
22.0	-8.25	-16.0	1.03 (14.28)	12.18 (0.00)	

c

MNI coordinate			Z-score (percentile)		Brain region
x	y	z	Basel	Neurosynth	Right lingual gyrus
19.25	-55.0	-8.0	0.81 (19.80)	4.60×10^{-3} (1.21)	

Figure 4. Example of Neurosynth map and point-to-point comparison.

(a) Visualization of Neurosynth association map of term ‘arousal’. Threshold: FWER < 0.05 (equivalent to absolute Z > 4.28). **(b-c)** Z-scores comparison of the same voxel in the second-level analysis results toward high vs. low arousal and Neurosynth map based on the term ‘arousal’. The percentile represents the score below which a particular percentage of the Z-score distribution in this map falls. **(b)** A voxel of a cluster from the right amygdala. **(c)** A voxel from the right lingual gyrus. FWER, family-wise error rate. Amyg, amygdala. RG, rectus gyrus. Note that Z-scores in Neurosynth association maps represent the degree of consistency between the study involving a given term and voxel activations, thus cannot be directly compared with Z-scores in the activation maps.

Predicting emotion rating and memory performance via MVPA

I established a framework of MVPA, expecting to decode emotional valence, arousal, and the performance of free recall and recognition in a single trial level via the fMRI signal in the picture encoding task. Considering the potential overfitting problem, that is, containing more parameters

than the data can justify, I used feature selection techniques based on the 'top-voxel' in the second-level analysis result, Neurosynth maps, and ICA result to extract possibly representative voxels from the whole brain. The selected 100 features were used to train SVM with RBF kernel. MVPA models fine-tuned by Grid search were applied to the test sets to obtain classification metrics with test accuracy.

The top hits in Neurosynth maps failed to decode all the prediction domains, where the accuracies were not far departed from the chance level (multi-way ANOVA, difference in means (MD) = 0.52, adjusted $p = 0.16$), suggesting that Neurosynth maps lack the brain region references in emotional and memory processes (Fig. 5a-e). In contrast, ‘top-voxel’- and ICA-based predictors relying on real data always showed significantly higher accuracy than chance level (multi-way ANOVA; ‘top-voxel’: MD = 4.92, adjusted $p = 5.06\times10^{-13}$; ICA: MD = 3.86, adjusted $p = 5.06\times10^{-13}$), except for the failed predictions on free recall (Fig. 5d; ‘top-voxel’: MD = 1.05, adjusted $p = 0.95$, multi-way ANOVA).

In addition, features obtained by the ‘top-voxel’ approach may render higher predictive information than independent components (multi-way ANOVA, MD = 1.01, adjusted $p = 5.33\times10^{-13}$). By checking the decoding tasks for all domains, the predictive ability of SVM is generally more powerful than that of simple GLM (multi-way ANOVA, MD = 0.77, adjusted $p = 3.05\times10^{-11}$), though its accuracy and sensitivity still have deficiencies (Fig. 5f).

In sum, brain region information suggested by real fMRI data contain information to predict emotion and memory on a single trial basis, thus possessing potential in prediction. However, the meta-analysis results provided by Neurosynth seem to be invalid for decoding emotion and memory.

a

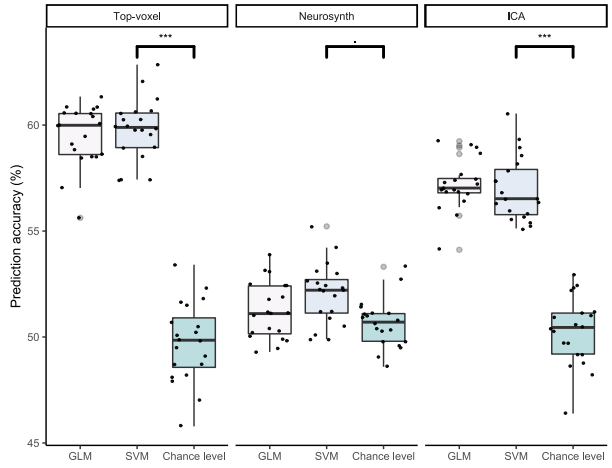

b

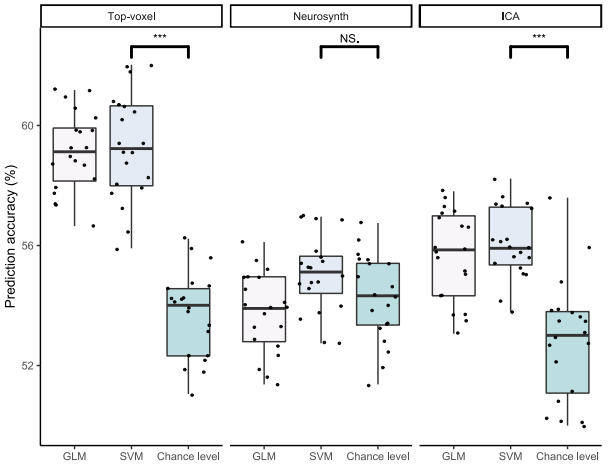

c

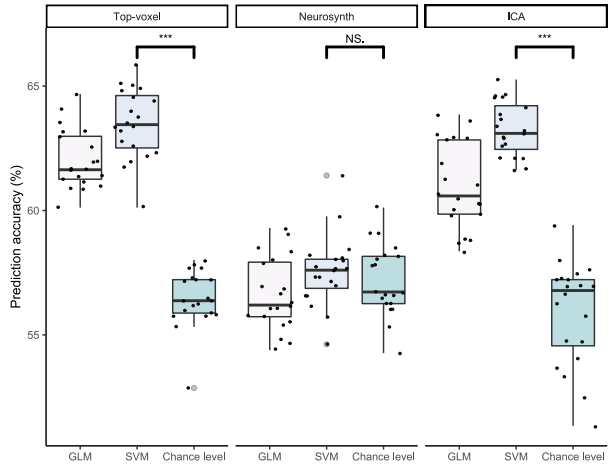

d

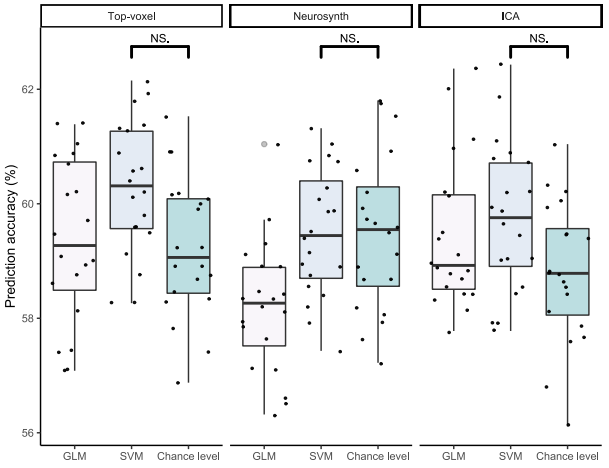

e

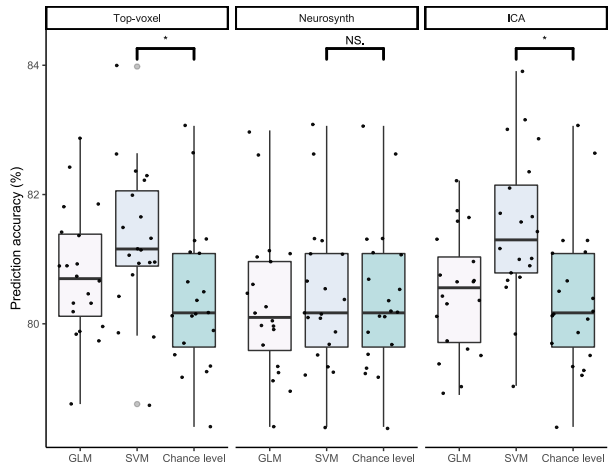

f

	precision	recall	f1-score	support
0	0.66	0.84	0.74	490
1	0.66	0.42	0.51	365
accuracy			0.66	855
macro avg	0.66	0.63	0.62	855
weighted avg	0.66	0.66	0.64	855

Figure 5. Predictive performances of MVPA models.

Figure 5. Predictive performances of MVPA models.

Test accuracies in decoding individual emotional **(a-b)** valence, **(c)** arousal, **(d)** free recall, and **(e)** recognition with various feature selection techniques. **(a)** Positive vs. neutral valence. Comparisons made by two-way ANOVA. **(b)** Negative vs. neutral valence. Comparisons made by two-way ANOVA. **(c)** High vs. low arousal. Comparisons made by two-way ANOVA. **(d)** Remembered vs. not-remembered. Comparisons made by two-way ANOVA. **(e)** Old vs. relatively new. Comparisons made by ordinal cumulative probability model. **(f)** Classification metric of high vs. low arousal prediction by SVM as an example. *** $p < 0.001$, ** $p < 0.01$, * $p < 0.05$, . $p < 0.1$. GLM, general linear model (logistic regression here). ICA, independent component analysis. NS., not significant. avg, averages.

Distributed patterns of activity in the cortical areas provide better prediction of cognitive states

Given the differences in the performance of the MVPA model given by different feature selection techniques, it is worth observing the brain regions where the voxels used for model training are located. The voxels rendered by the 'top-voxel' approach enabled the MVPA models to show significantly higher-than-chance level accuracy, indicating that the related brain regions may contribute to the prediction of emotion or memory process. However, the top hits in Neurosynth maps have low predictive power, and the associated brain regions may not be responsible for specific cognitive states, or the intensity of activity may be lower than other regions.

Multiple cortical areas, including the superior frontal gyrus (SFG) and occipitotemporal areas, were informative in the prediction task of emotional valence, while primary somatosensory and motor cortices also appeared to be involved in negative valence decoding (Table 4). In contrast, voxels concentrated in the limbic system provided by Neurosynth maps, where considerable voxels were located in the amygdala, did not contribute to the prediction (Table 4, Fig. 5a & 5b).

The primary somatosensory and motor cortices, as well as the occipitotemporal areas, were involved in predicting emotional arousal, all of which focused on the cerebral cortex (Table 4). Instead, Neurosynth ranks the amygdala as the most associated brain region in the term 'arousal', but with no significant effect on prediction (Table 4, Fig. 5c).

The parietal, temporal, and occipital lobes all seem to be involved in the prediction of subsequent recognition memory performance (Table 4). Nevertheless, Neurosynth gave many voxels concentrated in the fusiform gyri, which was considered slightly more associated with recognition than the limbic system, although the latter was still recommended as significant by Neurosynth (Table 4).

In a nutshell, many focused areas in the human cerebral cortex may be involved in emotional processing and memory encoding with more intensive activity. However, the amygdala, thought to be central to emotional processing, and the hippocampus, responsible for memory encoding, and the widespread activity pattern of individual cortical areas were not predictive of the cognitive states involved in the picture encoding task.

Predictive brain regions	Hemisphere	Voxel count	Peak MNI coordinates			Peak statistics		Feature selection techniques
			X	Y	Z	Z-score	$P_{nominal}$	
Positive vs. neutral valence								
Superior frontal gyrus (prefrontal cortex)	Left	8	-19.25	60.5	20	3.06	0.0022	'Top-voxel' approach
Middle occipital gyrus	Right	7	13.75	-90.75	4	3.99	0.0001	'Top-voxel' approach
Lingual gyrus	Left	6	-13.75	-71.5	-8	3.34	0.0008	'Top-voxel' approach
Middle occipital gyrus	Left	6	-38.5	-68.75	16	-2.28	0.0224	'Top-voxel' approach
Inferior occipital gyrus	Right	6	13.75	-88	-8	2.73	0.0064	'Top-voxel' approach
Amygdala	Right	45	22	-8.25	-16	12.18	0.0000	Neurosynth-guided
	Left	37	-24.75	-2.75	-20	11.86	0.0000	Neurosynth-guided
Uncinate fasciculus	Left	4	-27.5	2.75	-16	8.91	0.0000	Neurosynth-guided
Hippocampus	Right	3	22	-8.25	-20	10.78	0.0000	Neurosynth-guided
Parahippocampal gyrus	Left	3	-27.5	2.75	-24	8.65	0.0000	Neurosynth-guided
Negative vs. neutral valence								
Superior frontal gyrus (prefrontal cortex)	Right	8	0	49.5	16	2.68	0.0074	'Top-voxel' approach
Fusiform gyrus	Left	6	-33	-77	-16	2.18	0.0294	'Top-voxel' approach
Postcentral gyrus	Left	6	-52.25	-11	20	-1.88	0.0602	'Top-voxel' approach
Precentral gyrus	Right	6	5.5	-16.5	56	-1.26	0.2062	'Top-voxel' approach
	Left	5	-33	-11	64	-0.60	0.5506	'Top-voxel' approach
Amygdala	Left	42	-19.25	-2.75	-16	9.61	0.0000	Neurosynth-guided
	Right	39	19.25	-2.75	-20	12.19	0.0000	Neurosynth-guided
Parahippocampal gyrus	Left	6	-27.5	2.75	-24	7.91	0.0000	Neurosynth-guided
Hippocampus	Right	2	22	-8.25	-20	8.48	0.0000	Neurosynth-guided
Entorhinal area	Right	2	19.25	-2.75	-24	7.54	0.0000	Neurosynth-guided
High vs. low arousal								
Precentral gyrus	Right	12	22	-19.25	68	-2.14	0.0324	'Top-voxel' approach
Postcentral gyrus	Right	7	38.5	-27.5	64	-2.25	0.0243	'Top-voxel' approach
	Left	6	-52.25	-8.25	16	-2.13	0.0330	'Top-voxel' approach
Lingual gyrus	Right	6	13.75	-74.25	-12	3.80	0.0001	'Top-voxel' approach
Fusiform gyrus	Right	5	22	-74.25	-8	3.13	0.0017	'Top-voxel' approach
Amygdala	Right	43	19.25	-2.75	-16	10.54	0.0000	Neurosynth-guided
	Left	31	-22	0	-24	8.32	0.0000	Neurosynth-guided
Gyrus rectus	Left	8	-5.5	33	-16	7.11	0.0000	Neurosynth-guided
Cerebral peduncle	Right	3	19.25	-13.75	-8	6.66	0.0000	Neurosynth-guided
Uncinate fasciculus	Left	3	-30.25	0	-20	6.13	0.0000	Neurosynth-guided
Remembered vs. not-remebered								
Lingual gyrus	Right	9	11	-82.5	-8	2.62	0.0088	'Top-voxel' approach
Cuneus	Left	8	-2.75	-71.5	8	2.42	0.0157	'Top-voxel' approach
Middle occipital gyrus	Right	7	13.75	-90.75	8	2.95	0.0032	'Top-voxel' approach
Lingual gyrus	Left	7	-13.75	-71.5	-8	3.34	0.0008	'Top-voxel' approach
Middle frontal gyrus (posterior segment)	Left	7	-27.5	19.25	52	2.76	0.0058	'Top-voxel' approach

Hippocampus	Right	14	33	-22	-16	7.13	0.0000	Neurosynth-guided
Parahippocampal gyrus	Left	12	-27.5	-33	-8	8.58	0.0000	Neurosynth-guided
Fusiform gyrus	Left	11	-22	-33	-16	7.31	0.0000	Neurosynth-guided
Parahippocampal gyrus	Right	9	19.25	-27.5	-8	6.86	0.0000	Neurosynth-guided
Cingulum (hippocampus)	Right	9	24.75	-27.5	-12	7.39	0.0000	Neurosynth-guided
Old vs. familiar-new								
Angular gyrus	Left	8	-49.5	-63.25	28	1.49	0.1372	'Top-voxel' approach
Fusiform gyrus	Right	7	24.75	-71.5	-16	1.13	0.2597	'Top-voxel' approach
Pre-cuneus	Left	5	-2.75	-63.25	20	0.06	0.9514	'Top-voxel' approach
	Right	5	2.75	-38.5	40	0.99	0.3239	'Top-voxel' approach
Middle occipital gyrus	Left	5	-16.5	-96.25	8	-0.57	0.5679	'Top-voxel' approach
Fusiform gyrus	Left	47	-41.25	-41.25	-24	9.94	0.0000	Neurosynth-guided
	Right	32	41.25	-46.75	-20	8.77	0.0000	Neurosynth-guided
Posterior inferior temporal gyrus	Left	9	-44	-46.75	-20	8.62	0.0000	Neurosynth-guided
	Right	4	46.75	-55	-20	7.16	0.0000	Neurosynth-guided
Cerebellum	Left	4	-38.5	-44	-24	8.29	0.0000	Neurosynth-guided

Table 4. Summary of the voxels selected in MVPA model training.

The five regions with the highest voxel count in each domain prediction and feature selection technique ('top-voxel' or Neuorsynth-guided approach) were listed. The nominal *p* values were queried from the Z table. Note that Z-scores, *p*-values, and voxel counts corresponding to different feature selection techniques are not comparable.

Discussion

By using GLM-based brain mapping and SVM-based MVPA, the results indicate cortical representations of memory retrieval processes and emotions, also the potential and limitations for predicting individual subjects' single-trial performance. Current MVPA models perform negligibly on the prediction task of individual free recall performance but show adequate predictive ability in decoding emotional dimensions and recognition memory, with higher accuracy in emotion prediction than in memory. Compared with the limbic system signal-based predictions guided by the meta-analysis results from Neurosynth, I extended the MVPA of complex cognitive states to distributed cortical representations, demonstrating the bias of previous studies on brain regions responsible for emotion and memory.

Brain region representations of the emotional dimensions and memory processes

In the second-level analysis results of fMRI signals from the encoding task, emotional and memory-related phenotypes can be projected to various distributed activation patterns in cortical regions. The prediction results of MVPA based on SVM also supported the distributional assumption of neural representations of emotion and memory, compared with the multivariate linear regression that assumed independence of features. Given the necessity of multiple comparison corrections for fMRI activation maps, no voxels survived the Bonferroni correction in this experiment, requiring a larger sample size to increase the statistical power (Poldrack *et al.*, 2008). The lack of significant voxels may be because the information in the IAPS pictures was much more complex and noisier than the single variable in a controlled experiment. However, many researchers argued that the voxels with uncorrected p-value should still be reported, which could provide insights for future research and meta-analyses (Poldrack *et al.*, 2008).

The brain regions I report that may be associated with emotional and memory-related phenotypes are partly consistent with previous studies, many of which are located in the occipital lobe, the visual processing center of the human brain (Rehman and Al Khalili, 2023). The IOG is connected to the amygdala and is involved in processing human faces and emotionally important visual stimuli (Sato *et al.*, 2017). A correlation was found between left IOG activation and unpleasant pictures, but its correlation with positive valence was not evident in previous studies (Geday *et al.*, 2003; Nielen *et al.*, 2009). The right MOG presents a preference for visuospatial processing, but few studies have detected its association with positive valence (Nielen *et al.*, 2009; Rosengarth *et al.*, 2021). The LG is active in global shape processing, and its activation is related to the encoding of complex objects and arousal, consistent with its activation in predicting arousal rating and memory performances

(Mechelli *et al.*, 2000; Mather *et al.*, 2006; Slotnick and Schacter, 2006).

The left hemispheric dominance of recognition memory is uncommon in previous studies of emotional memory, while face recognition may have an advantage in the right hemisphere instead. However, some studies report that the left hemisphere advantage may be manifested in recognition experiments involving analytical judgment, which may be related to the function of the left FuG in judging similar objects by their structure (Sergent and Bindra, 1981; Kellenbach *et al.*, 2005).

The left FuG is also responsible for visual word processing and may be involved in the interplay between the recognition memory of pictures and semantic memory (Dehaene and Cohen, 2011). The subjects may name the pictures in the encoding task and integrate visual information into the schema for better performance, which may be a means of consciously or subconsciously learning visual content. In fact, one study has found that pairing facial actions with words can affect subsequent memory, supporting the memory strategy human may adopt (Doyle and Lindquist, 2018).

In this experiment, the activity of the subcortical regions of the limbic system was not significant, which seemed inconsistent with its central role in emotional and memory processing in popular ideas. I would hasten to point out that the formulation of this idea should not be interpreted broadly while ignoring the specific activity patterns of the limbic system in the distributed neural systems of different cognitive processes. Although the hippocampus is essential in episodic memory encoding, many studies have failed to detect hippocampal activity during memory retrieval (Wagner *et al.*, 1998; Fernández *et al.*, 1999; Reas and Brewer, 2013). Given that the analysis I performed used the fMRI signal from the picture encoding task to predict the performances during subsequent retrieval stages, the strength of memory on a single trial may be more focused on cortical representations. In addition, I would try second-level analyses of the fMRI signal from the picture recognition task to perform the brain mapping of free recall and recognition. Turning to the aspect of the amygdala, its exact role in the emotional processing of visual stimuli is unclear but strongly associated with fear and appears to be independent of the recognition of other basic emotions such as sadness, happiness, and disgust (Geday *et al.*, 2003; Sato *et al.*, 2004). Distinct neural systems may mediate the recognition of different types of emotions (Geday *et al.*, 2003). Brain mapping of the dimensional model is an issue that future research could focus on to investigate whether the psychological concept can be well reduced to the neural basis.

A call for cautious use of SVC and term registration

Inconsistent with the results of the second-level analysis of the fMRI data in the encoding task, the terms related to emotion and memory in Neurosynth are strongly associated with the activities of the subcortical regions in the limbic system, such as the hippocampus and amygdala. The activity

pattern of the limbic system does not seem to predict emotion and memory in MVPA, indicating that previous fMRI studies analyzed by Neurosynth are biased toward the limbic system, which may be due to the incautious approach taken by some studies in processing and reporting activation maps to control the threshold of multiple comparisons correction using SVC for regions in the limbic system rather than whole-brain analysis (Gottfried *et al.*, 2004; van Eijndhoven *et al.*, 2011). Although lowering the statistical threshold can provide potential insights for brain mapping, when biased brain region information is used as the basis for statistical inference or machine learning, such as MVPA, this will severely impair model performance and mislead future studies of neural representations of cognitive functions. In Neurosynth terms such as recognition, larger brain regions (such as FuG) are thought to be associated with cognitive concepts instead of small clusters of voxels that occupy limited parts of a brain region. This pattern may reflect the assumption of functional homogeneity of one brain region in many ROI-based studies and the use of poorly defined or unregistered brain regions as ROIs, even though different parts within a single brain region can exhibit distinctly different activity patterns (Poldrack, 2007; Hong *et al.*, 2019). Because of the increase in large-sample fMRI studies and the innovations in whole-brain error control methods, I recommend using SVC for ROIs with caution in functional neuroimaging experiments and reporting significant voxels with the registered atlas used (Genovese *et al.*, 2002; Worsley *et al.*, 2004; Poldrack *et al.*, 2009; Poldrack, 2012).

In the context of different disciplines, there may be polysemy in term use. In this article, arousal refers to a dimension in the dimensional model of emotion. However, in neurobiology and sometimes in daily use, arousal represents the physiological and psychological state of wakefulness-sleep, activated by the ascending reticular activation system (ARAS) (Jones, 2008). The association map for the arousal term from Neurosynth reflects activity in the amygdala rather than brainstem and hypothalamic nuclei, suggesting that the term refers to emotional arousal. Therefore, pre-registering terms with precise biological definitions in neuroimaging databases can be considered to avoid confusion and guide ROI-based studies.

On the comparison of approaches, input features, and model performance of MVPA

The SVM-based MVPA model showed slightly higher decoding accuracy than GLM, which proves its superiority. Although the inclusion of interaction terms in GLM can reflect the joint effect of multiple voxels, the large number of voxels in the MVPA task will lead to a combinatorial explosion in the number of explanatory variables. The theoretically infinite-dimensional feature space of the RBF kernel happens to be consistent with the assumption of distributive activity patterns of cognitive processes (Shashua, 2009). In addition, I adopted ICA-based MVPA only for exploratory purposes in this experiment, and the reason for the inferiority to the ‘top-voxel’ approach is unclear. No studies

have systematically examined ICA performance in group comparison on event-related tasks (Rombouts *et al.*, 2009; Schöpf *et al.*, 2011; Mahmoudi *et al.*, 2012). Due to time constraints, I did not inspect the difference between the brain region representations of ICA-based and 'top-voxel' approaches from the probabilistic map reflecting the loading of ICs. Future work may focus on the distribution of features selected by the ICA-based approach in different tasks.

In view of the non-linear transformation of input features by SVM-based MVPA, the contribution of 'top voxels' in the activation maps and top hits in Neurosynth maps cannot be detected one by one, and the predictive accuracy can only reflect the combined effect of voxels. In addition to the brain regions revealed by brain mapping results, SFG, PrCG, and postcentral gyrus (PoCG) are also involved in decoding cognitive states, consistent with previous studies. Correlations were found for positive valence with left SFG and negative valence with right SFG (Habes *et al.*, 2013; Falquez *et al.*, 2014). The PoCG, where the primary somatosensory cortex lies, is sensitive to negative valence auditory and visual stimuli and is related to sexual arousal (Hu *et al.*, 2008; Gu *et al.*, 2019). The right PrCG is associated with physiological factors during visually mediated sexual arousal (Seok *et al.*, 2016).

In this study, MVPA models did not successfully predict individual free recall performance. Furthermore, the models decoding emotional dimensions and recognition memory performance also have room for improvement. Relatively poor model performances may be related to the insufficient number of features used for prediction, which is difficult to determine. In addition to incorporating more features into the MVPA model, data containing more samples would be available to increase the statistical power of brain mapping and MVPA decoding performance once we solve the cluster computing issue with the University of Basel. Although the long-term utility of artificial neural networks (ANNs) in MVPA has not been fully proven, given its potential to mine fine-grained features in fMRI data, I would try to use an ANN-based MVPA framework to predict the cognitive contents (Kuntzelman *et al.*, 2021).

Conclusion

In conclusion, the study successfully predicted the individual recognition memory and emotional dimensions in the picture tasks using fMRI signals based on cortical regions, supporting the theory of distributive neural representation alliances in the memory retrieval processes. In addition, the failure of MVPA models using primarily amygdala and hippocampus signals in cognitive state decoding tasks suggests the pitfalls of SVC for statistical control with the imprecise definition of ROIs. I appeal to the neuroimaging community to use SVC carefully and to indicate the pre-registered brain region definition in ROI-based analysis. Although the MVPA models did not achieve very high

accuracy predictions, increasing the number of features and the sample size is expected to improve decoding performance. Finally, the advances in predicting episodic memory performance and emotional regulation can enhance our understanding of the mechanism underlying memory and emotional processes, provide directions for psychiatric research, and could have a major impact on the translation of brain-computer interfaces.

References

AGUIRRE, G. K., ZARAHN, E. AND D'ESPOSITO, M. (1998) The variability of human, BOLD hemodynamic responses., *NeuroImage*. United States, 8(4), pp. 360–369. doi: 10.1006/nimg.1998.0369.

BAIER, B., STOETER, P. AND DIETERICH, M. (2009) Anatomical correlates of ocular motor deficits in cerebellar lesions., *Brain : a journal of neurology*. England, 132(Pt 8), pp. 2114–2124. doi: 10.1093/brain/awp165.

BEN-HUR, A., ONG, C. S., SONNENBURG, S., SCHÖLKOPF, B. AND RÄTSCH, G. (2008) Support vector machines and kernels for computational biology., *PLoS computational biology*. United States, 4(10), p. e1000173. doi: 10.1371/journal.pcbi.1000173.

BRADLEY, M. M. AND LANG, P. J. (2007) The International Affective Picture System (IAPS) in the study of emotion and attention., in *Handbook of emotion elicitation and assessment.* Bradley, Margaret M.: NIMH Center for the Study of Emotion and Attention (CSEA), University of Florida, Box 112766 HSC, Gainesville, FL, US, 32610-0165: Oxford University Press (Series in affective science.), pp. 29–46.

BROCA, P. (1861) *Bulletins de la Société d'anthropologie de Paris. Perte de la parole, ramollissement chronique et destruction partielle du lobe antérieur gauche du cerveau*, *TA - TT* -. Paris SE -: Librarie Victor Masson. doi: LK - https://worldcat.org/title/861230165. English translation: https://psychclassics.yorku.ca/Broca/perte-e.htm.

CAHILL, L., BABINSKY, R., MARKOWITSCH, H. J. AND MCGAUGH, J. L. (1995) The amygdala and emotional memory, *Nature*, 377(6547), pp. 295–296. doi: 10.1038/377295a0.

CALDER, A. J., LAWRENCE, A. D. AND YOUNG, A. W. (2001) Neuropsychology of fear and loathing., *Nature reviews. Neuroscience*. England, 2(5), pp. 352–363. doi: 10.1038/35072584.

CALLICOTT, J. H., RAMSEY, N. F., TALLENT, K., BERTOLINO, A., KNABLE, M. B., COPPOLA, R., GOLDBERG, T., VAN GELDEREN, P., MATTAY, V. S., FRANK, J. A., MOONEN, C. T. W. AND WEINBERGER, D. R. (1998) Functional Magnetic Resonance Imaging Brain Mapping in Psychiatry: Methodological Issues Illustrated in a Study of Working Memory in Schizophrenia, *Neuropsychopharmacology*, 18(3), pp. 186–196. doi: 10.1016/S0893-133X(97)00096-1.

CHUMBLEY, J. R. AND FRISTON, K. J. (2009) False discovery rate revisited: FDR and topological inference using Gaussian random fields., *NeuroImage*. United States, 44(1), pp. 62–70. doi: 10.1016/j.neuroimage.2008.05.021.

DEHAENE, S. AND COHEN, L. (2011) The unique role of the visual word form area in reading., *Trends in cognitive sciences*. England, 15(6), pp. 254–262. doi: 10.1016/j.tics.2011.04.003.

DOUCET, G., SKIDMORE, C., EVANS, J., SHARAN, A., SPERLING, M., PUSTINA, D. AND TRACY, J. (2014) Temporal Lobe Epilepsy and Surgery Selectively Alter the Dorsal, Not the Ventral, Default-Mode Network, *Frontiers in Neurology*, 5. doi: 10.3389/fneur.2014.00023.

DOYLE, C. M. AND LINDQUIST, K. A. (2018) When a word is worth a thousand pictures: Language shapes perceptual memory for emotion., *Journal of Experimental Psychology: General*. Lindquist, Kristen A.: Department of Psychology and Neuroscience, University of North Carolina, Chapel Hill, Davie Hall 321, Chapel Hill, NC, US, 27510, Kristen.lindquist@unc.edu: American Psychological Association, 147, pp. 62–73. doi: 10.1037/xge0000361.

DRONKERS, N. F., PLAISANT, O., IBA-ZIZEN, M. T. AND CABANIS, E. A. (2007) Paul Broca's historic cases: high resolution MR imaging of the brains of Leborgne and Lelong, *Brain*, 130(5), pp. 1432–1441. doi: 10.1093/brain/awm042.

DUBOIS, J., OYA, H., TYSZKA, J. M., HOWARD, M. 3RD, EBERHARDT, F. AND ADOLPHS, R. (2020) Causal mapping of emotion networks in the human brain: Framework and initial findings., *Neuropsychologia*. England, 145, p. 106571. doi: 10.1016/j.neuropsychologia.2017.11.015.

VAN EIJNDHOVEN, P., VAN WINGEN, G., FERNÁNDEZ, G., RIJPKEMA, M., VERKES, R. J., BUITELAAR, J. AND TENDOLKAR, I. (2011) Amygdala responsivity related to memory of emotionally neutral stimuli constitutes a trait factor for depression, *NeuroImage*, 54(2), pp. 1677–1684. doi: https://doi.org/10.1016/j.neuroimage.2010.08.040.

EVANS, A. C., COLLINS, D. L., MILLS, S. R., BROWN, E. D., KELLY, R. L. AND PETERS, T. M. (1993) 3D statistical neuroanatomical models from 305 MRI volumes, in *1993 IEEE Conference Record Nuclear Science Symposium and Medical Imaging Conference*, pp. 1813–1817 vol.3. doi: 10.1109/NSSMIC.1993.373602.

EYSENCK, M. (2012) *Attention and arousal: Cognition and performance*. Springer Science & Business Media.

FALQUEZ, R., COUTO, B., IBANEZ, A., FREITAG, M. T., BERGER, M., ARENS, E. A., LANG, S. AND BARNOW, S. (2014) Corrigendum: Detaching from the negative by reappraisal: the role of right superior frontal gyrus (BA9/32)., *Frontiers in Behavioral Neuroscience*. doi: 10.3389/fnbeh.2014.00264.

FARIA, A. V, JOEL, S. E., ZHANG, Y., OISHI, K., VAN ZJIL, P. C. M., MILLER, M. I., PEKAR, J. J. AND MORI, S. (2012) Atlas-based analysis of resting-state functional connectivity: evaluation for reproducibility and multi-modal anatomy-function correlation studies., *NeuroImage*. United States, 61(3), pp. 613–621. doi: 10.1016/j.neuroimage.2012.03.078.

FERNANDES, M. A., MOSCOVITCH, M., ZIEGLER, M. AND GRADY, C. (2005) Brain regions associated with successful and unsuccessful retrieval of verbal episodic memory as revealed by divided attention., *Neuropsychologia*. England, 43(8), pp. 1115–1127. doi:

10.1016/j.neuropsychologia.2004.11.026.

FERNÁNDEZ, G., EFFERN, A., GRUNWALD, T., PEZER, N., LEHNERTZ, K., DÜMPELMANN, M., VAN ROOST, D. AND ELGER, C. E. (1999) Real-time tracking of memory formation in the human rhinal cortex and hippocampus., *Science (New York, N.Y.)*. United States, 285(5433), pp. 1582–1585. doi: 10.1126/science.285.5433.1582.

FOX, P. T., MINTUN, M. A., RAICHLE, M. E., MIEZIN, F. M., ALLMAN, J. M. AND VAN ESSEN, D. C. (1986) Mapping human visual cortex with positron emission tomography, *Nature*, 323(6091), pp. 806–809. doi: 10.1038/323806a0.

FRANKLAND, P. W. AND BONTEMPI, B. (2005) The organization of recent and remote memories., *Nature reviews. Neuroscience*. England, 6(2), pp. 119–130. doi: 10.1038/nrn1607.

FRISTON, K. J., HOLMES, A. P., PRICE, C. J., BÜCHEL, C. AND WORSLEY, K. J. (1999) Multisubject fMRI studies and conjunction analyses., *NeuroImage*. United States, 10(4), pp. 385–396. doi: 10.1006/nimg.1999.0484.

GEDAY, J., GJEDDE, A., BOLDSEN, A.-S. AND KUPERS, R. (2003) Emotional valence modulates activity in the posterior fusiform gyrus and inferior medial prefrontal cortex in social perception, *NeuroImage*, 18(3), pp. 675–684. doi: https://doi.org/10.1016/S1053-8119(02)00038-1.

GENOVESE, C. R., LAZAR, N. A. AND NICHOLS, T. (2002) Thresholding of statistical maps in functional neuroimaging using the false discovery rate., *NeuroImage*. United States, 15(4), pp. 870–878. doi: 10.1006/nimg.2001.1037.

GOTTFRIED, J. A., SMITH, A. P. R., RUGG, M. D. AND DOLAN, R. J. (2004) Remembrance of odors past: human olfactory cortex in cross-modal recognition memory., *Neuron*. United States, 42(4), pp. 687–695. doi: 10.1016/s0896-6273(04)00270-3.

GREICIUS, M. D., KRASNOW, B., REISS, A. L. AND MENON, V. (2003) Functional connectivity in the resting brain: a network analysis of the default mode hypothesis., *Proceedings of the National Academy of Sciences of the United States of America*. United States, 100(1), pp. 253–258. doi: 10.1073/pnas.0135058100.

GU, J., CAO, L. AND LIU, B. (2019) Modality-general representations of valences perceived from visual and auditory modalities, *NeuroImage*, 203, p. 116199. doi: https://doi.org/10.1016/j.neuroimage.2019.116199.

HABES, I., KRALL, S. C., JOHNSTON, S. J., YUEN, K. S. L., HEALY, D., GOEBEL, R., SORGER, B. AND LINDEN, D. E. J. (2013) Pattern classification of valence in depression., *NeuroImage. Clinical*. Netherlands, 2, pp. 675–683. doi: 10.1016/j.nicl.2013.05.001.

HARRELL, F. E. (2015) Ordinal Logistic Regression BT - Regression Modeling Strategies: With Applications to Linear Models, Logistic and Ordinal Regression, and Survival Analysis, in Harrell

Frank E., J. (ed.). Cham: Springer International Publishing, pp. 311–325. doi: 10.1007/978-3-319-19425-7_13.

HAXBY, J. V (2012) Multivariate pattern analysis of fMRI: the early beginnings., *NeuroImage*. United States, 62(2), pp. 852–855. doi: 10.1016/j.neuroimage.2012.03.016.

HONG, Y.-W., YOO, Y., HAN, J., WAGER, T. D. AND WOO, C.-W. (2019) False-positive neuroimaging: Undisclosed flexibility in testing spatial hypotheses allows presenting anything as a replicated finding., *NeuroImage*. United States, 195, pp. 384–395. doi: 10.1016/j.neuroimage.2019.03.070.

HU, S.-H., WEI, N., WANG, Q.-D., YAN, L.-Q., WEI, E.-Q., ZHANG, M.-M., HU, J.-B., HUANG, M.-L., ZHOU, W.-H. AND XU, Y. (2008) Patterns of brain activation during visually evoked sexual arousal differ between homosexual and heterosexual men., *AJNR. American journal of neuroradiology*. United States, 29(10), pp. 1890–1896. doi: 10.3174/ajnr.A1260.

HUTTON, C., JOSEPHS, O., STADLER, J., FEATHERSTONE, E., REID, A., SPECK, O., BERNARDING, J. AND WEISKOPF, N. (2011) The impact of physiological noise correction on fMRI at 7T, *NeuroImage*, 57(1), pp. 101–112. doi: https://doi.org/10.1016/j.neuroimage.2011.04.018.

JONES, B. E. (2008) Modulation of Cortical Activation and Behavioral Arousal by Cholinergic and Orexinergic Systems, *Annals of the New York Academy of Sciences*. John Wiley & Sons, Ltd, 1129(1), pp. 26–34. doi: https://doi.org/10.1196/annals.1417.026.

KELLENBACH, M. L., HOVIUS, M. AND PATTERSON, K. (2005) A pet study of visual and semantic knowledge about objects., *Cortex; a journal devoted to the study of the nervous system and behavior*. Italy, 41(2), pp. 121–132. doi: 10.1016/s0010-9452(08)70887-6.

KENSINGER E.A. (2004) Remembering Emotional Experiences: The Contribution of Valence and Arousal, *Reviews in the Neurosciences*, 15(4), pp. 241–252. doi: doi:10.1515/REVNEURO.2004.15.4.241.

KRAGEL, P. A. AND LABAR, K. S. (2016) Decoding the Nature of Emotion in the Brain., *Trends in cognitive sciences*. England, 20(6), pp. 444–455. doi: 10.1016/j.tics.2016.03.011.

KRIEGESKORTE, N. AND DOUGLAS, P. K. (2019) Interpreting encoding and decoding models., *Current opinion in neurobiology*. England, 55, pp. 167–179. doi: 10.1016/j.conb.2019.04.002.

KRIEGESKORTE, N., SIMMONS, W. K., BELLGOWAN, P. S. F. AND BAKER, C. I. (2009) Circular analysis in systems neuroscience: the dangers of double dipping., *Nature neuroscience*. United States, 12(5), pp. 535–540. doi: 10.1038/nn.2303.

KUNTZELMAN, K. M., WILLIAMS, J. M., LIM, P. C., SAMAL, A., RAO, P. K. AND JOHNSON, M. R. (2021) Deep-Learning-Based Multivariate Pattern Analysis (dMVPA): A Tutorial and a Toolbox , *Frontiers in Human Neuroscience* . Available at: https://www.frontiersin.org/articles/10.3389/fnhum.2021.638052.

LETTIERI, G., HANDJARAS, G., RICCIARDI, E., LEO, A., PAPALE, P., BETTA, M., PIETRINI, P. AND CECCHETTI, L. (2019) Emotionotopy in the human right temporo-parietal cortex., *Nature communications*. England, 10(1), p. 5568. doi: 10.1038/s41467-019-13599-z.

LUKSYS, G., FASTENRATH, M., COYNEL, D., FREYTAG, V., GSCHWIND, L., HECK, A., JESSEN, F., MAIER, W., MILNIK, A., RIEDEL-HELLER, S. G., SCHERER, M., SPALEK, K., VOGLER, C., WAGNER, M., WOLFSGRUBER, S., PAPASSOTIROPOULOS, A. AND DE QUERVAIN, D. J.-F. (2015) Computational dissection of human episodic memory reveals mental process-specific genetic profiles., *Proceedings of the National Academy of Sciences of the United States of America*. United States, 112(35), pp. E4939-48. doi: 10.1073/pnas.1500860112.

MAHMOUDI, A., TAKERKART, S., REGRAGUI, F., BOUSSAOUD, D. AND BROVELLI, A. (2012) Multivoxel pattern analysis for FMRI data: a review., *Computational and mathematical methods in medicine*. United States, 2012, p. 961257. doi: 10.1155/2012/961257.

MATHER, M., MITCHELL, K. J., RAYE, C. L., NOVAK, D. L., GREENE, E. J. AND JOHNSON, M. K. (2006) Emotional arousal can impair feature binding in working memory., *Journal of cognitive neuroscience*. United States, 18(4), pp. 614–625. doi: 10.1162/jocn.2006.18.4.614.

MECHELLI, A., HUMPHREYS, G. W., MAYALL, K., OLSON, A. AND PRICE, C. J. (2000) Differential effects of word length and visual contrast in the fusiform and lingual gyri during reading., *Proceedings. Biological sciences*. England, 267(1455), pp. 1909–1913. doi: 10.1098/rspb.2000.1229.

MORGANE, P. J., GALLER, J. R. AND MOKLER, D. J. (2005) A review of systems and networks of the limbic forebrain/limbic midbrain, *Progress in Neurobiology*, 75(2), pp. 143–160. doi: https://doi.org/10.1016/j.pneurobio.2005.01.001.

MUCKLI, L., NAUMER, M. J. AND SINGER, W. (2009) Bilateral visual field maps in a patient with only one hemisphere., *Proceedings of the National Academy of Sciences of the United States of America*. United States, 106(31), pp. 13034–13039. doi: 10.1073/pnas.0809688106.

NIELEN, M. M. A., HESLENFELD, D. J., HEINEN, K., VAN STRIEN, J. W., WITTER, M. P., JONKER, C. AND VELTMAN, D. J. (2009) Distinct brain systems underlie the processing of valence and arousal of affective pictures, *Brain and Cognition*, 71(3), pp. 387–396. doi: https://doi.org/10.1016/j.bandc.2009.05.007.

NOUR, M. AND LIEBESKIND, D. S. (2011) Brain imaging in stroke: insight beyond diagnosis., *Neurotherapeutics : the journal of the American Society for Experimental NeuroTherapeutics*. United States, 8(3), pp. 330–339. doi: 10.1007/s13311-011-0046-0.

OGAWA, S., TANK, D. W., MENON, R., ELLERMANN, J. M., KIM, S. G., MERKLE, H. AND UGURBIL, K. (1992) Intrinsic signal changes accompanying sensory stimulation: functional brain mapping with magnetic resonance imaging., *Proceedings of the National Academy of Sciences of the United States of*

America. United States, 89(13), pp. 5951–5955. doi: 10.1073/pnas.89.13.5951.

PATER, M. R. A., DORFER, T. A., GSCHWIND, L., COYNEL, D., PAPASSOTIROPOULOS, A., QUERVAIN, D. J. DE AND LUKSYS, G. (2018) Predicting Human Memory Performance through Multi-Voxel Pattern Analysis, in *Federation of European Neuroscience Societies*. Berlin.

PENNY, W., FRISTON, K., ASHBURNER, J., KIEBEL, S. AND NICHOLS, T. (2007) *Statistical Parametric Mapping: The Analysis of Functional Brain Images*. doi: 10.1016/B978-0-12-372560-8.X5000-1.

POLDRACK, R. A. (2007) Region of interest analysis for fMRI., *Social cognitive and affective neuroscience*. England, 2(1), pp. 67–70. doi: 10.1093/scan/nsm006.

POLDRACK, R. A. (2011) Inferring mental states from neuroimaging data: from reverse inference to large-scale decoding., *Neuron*. United States, 72(5), pp. 692–697. doi: 10.1016/j.neuron.2011.11.001.

POLDRACK, R. A. (2012) The future of fMRI in cognitive neuroscience., *NeuroImage*. United States, 62(2), pp. 1216–1220. doi: 10.1016/j.neuroimage.2011.08.007.

POLDRACK, R. A., FLETCHER, P. C., HENSON, R. N., WORSLEY, K. J., BRETT, M. AND NICHOLS, T. E. (2008) Guidelines for reporting an fMRI study., *NeuroImage*. United States, 40(2), pp. 409–414. doi: 10.1016/j.neuroimage.2007.11.048.

POLDRACK, R. A., HALCHENKO, Y. O. AND HANSON, S. J. (2009) Decoding the large-scale structure of brain function by classifying mental States across individuals., *Psychological science*. United States, 20(11), pp. 1364–1372. doi: 10.1111/j.1467-9280.2009.02460.x.

POLDRACK, R. A., MUMFORD, J. A. AND NICHOLS, T. E. (2011) *Handbook of Functional MRI Data Analysis*. Cambridge: Cambridge University Press. doi: DOI: 10.1017/CBO9780511895029.

RAJAH, M. N. AND D'ESPOSITO, M. (2005) Region-specific changes in prefrontal function with age: a review of PET and fMRI studies on working and episodic memory, *Brain*, 128(9), pp. 1964–1983. doi: 10.1093/brain/awh608.

REAS, E. T. AND BREWER, J. B. (2013) Effortful retrieval reduces hippocampal activity and impairs incidental encoding., *Hippocampus*. United States, 23(5), pp. 367–379. doi: 10.1002/hipo.22096.

REHMAN, A. AND AL KHALILI, Y. (2023) *Neuroanatomy, Occipital Lobe. [Updated 2022 Jul 25]*, *StatPearls [Internet]. Treasure Island (FL): StatPearls Publishing*. Available at: https://www.ncbi.nlm.nih.gov/books/NBK544320/ (Accessed: 30 April 2023).

RISSMAN, J. AND WAGNER, A. D. (2012) Distributed representations in memory: insights from functional brain imaging., *Annual review of psychology*. United States, 63, pp. 101–128. doi: 10.1146/annurev-psych-120710-100344.

ROMBOUTS, S. A. R. B., DAMOISEAUX, J. S., GOEKOOP, R., BARKHOF, F., SCHELTENS, P., SMITH, S. M.

AND BECKMANN, C. F. (2009) Model-free group analysis shows altered BOLD FMRI networks in dementia, *Human Brain Mapping*. John Wiley & Sons, Ltd, 30(1), pp. 256–266. doi: https://doi.org/10.1002/hbm.20505.

ROSENGARTH, K., KLEINJUNG, T., LANGGUTH, B., LANDGREBE, M., LOHAUS, F., GREENLEE, M. W., HAJAK, G., SCHMIDT, N. O. AND SCHECKLMANN, M. (2021) Altered brain responses to emotional facial expressions in tinnitus patients, in Langguth, B., Kleinjung, T., De Ridder, D., Schlee, W., and Vanneste, S. B. T.-P. in B. R. (eds) *Tinnitus - An Interdisciplinary Approach Towards Individualized Treatment: Towards understanding the complexity of tinnitus*. Elsevier, pp. 189–207. doi: https://doi.org/10.1016/bs.pbr.2021.01.026.

RUSSELL, J. A. (1980) A circumplex model of affect., *Journal of personality and social psychology*. American Psychological Association, 39(6), p. 1161.

SATO, W., KOCHIYAMA, T., UONO, S., MATSUDA, K., USUI, K., USUI, N., INOUE, Y. AND TOICHI, M. (2017) Bidirectional electric communication between the inferior occipital gyrus and the amygdala during face processing., *Human brain mapping*. United States, 38(9), pp. 4511–4524. doi: 10.1002/hbm.23678.

SATO, W., KOCHIYAMA, T., YOSHIKAWA, S., NAITO, E. AND MATSUMURA, M. (2004) Enhanced neural activity in response to dynamic facial expressions of emotion: an fMRI study, *Cognitive Brain Research*, 20(1), pp. 81–91. doi: https://doi.org/10.1016/j.cogbrainres.2004.01.008.

SCHACTER, D. L. (2008) *Searching for memory: The brain, the mind, and the past*. Basic books.

SCHACTER, D. L., GILBERT, D. T. AND WEGNER, D. M. (2009) *Psychology*. Macmillan.

SCHÖPF, V., WINDISCHBERGER, C., ROBINSON, S., KASESS, C. H., FISCHMEISTER, F. P., LANZENBERGER, R., ALBRECHT, J., KLEEMANN, A. M., KOPIETZ, R., WIESMANN, M. AND MOSER, E. (2011) Model-free fMRI group analysis using FENICA, *NeuroImage*, 55(1), pp. 185–193. doi: https://doi.org/10.1016/j.neuroimage.2010.11.010.

SEOK, J.-W., SOHN, J.-H. AND CHEONG, C. (2016) Neural substrates of sexual arousal in heterosexual males: event-related fMRI investigation, *Journal of Physiological Anthropology*, 35(1), p. 8. doi: 10.1186/s40101-016-0089-3.

SERGENT, J. AND BINDRA, D. (1981) Differential hemispheric processing of faces: Methodological considerations and reinterpretation., *Psychological Bulletin*. US: American Psychological Association, pp. 541–554. doi: 10.1037/0033-2909.89.3.541.

SHASHUA, A. (2009) Introduction to Machine Learning: Class Notes 67577, *arXiv e-prints*, p. arXiv:0904.3664. doi: 10.48550/arXiv.0904.3664.

SIDDIQI, S. H., KORDING, K. P., PARVIZI, J. AND FOX, M. D. (2022) Causal mapping of human brain function., *Nature reviews. Neuroscience*. England, 23(6), pp. 361–375. doi: 10.1038/s41583-022-

00583-8.

SLOTNICK, S. D. AND SCHACTER, D. L. (2006) The nature of memory related activity in early visual areas, *Neuropsychologia*, 44(14), pp. 2874–2886. doi: https://doi.org/10.1016/j.neuropsychologia.2006.06.021.

STUDENT (1908) The Probable Error of a Mean, *Biometrika*. [Oxford University Press, Biometrika Trust], 6(1), pp. 1–25. doi: 10.2307/2331554.

TULVING, E. (2002) Episodic memory: from mind to brain., *Annual review of psychology*. United States, 53, pp. 1–25. doi: 10.1146/annurev.psych.53.100901.135114.

VIGNANDO, M., FFYTCHE, D., LEWIS, S. J. G., LEE, P. H., CHUNG, S. J., WEIL, R. S., HU, M. T., MACKAY, C. E., GRIFFANTI, L., PINS, D., DUJARDIN, K., JARDRI, R., TAYLOR, J.-P., FIRBANK, M., MCALONAN, G., MAK, H. K. F., HO, S. L. AND MEHTA, M. A. (2022) Mapping brain structural differences and neuroreceptor correlates in Parkinson's disease visual hallucinations, *Nature Communications*, 13(1), p. 519. doi: 10.1038/s41467-022-28087-0.

WAGNER, A. D., SCHACTER, D. L., ROTTE, M., KOUTSTAAL, W., MARIL, A., DALE, A. M., ROSEN, B. R. AND BUCKNER, R. L. (1998) Building memories: remembering and forgetting of verbal experiences as predicted by brain activity., *Science (New York, N.Y.)*. United States, 281(5380), pp. 1188–1191. doi: 10.1126/science.281.5380.1188.

WORSLEY, K. J., LIAO, C. H., ASTON, J., PETRE, V., DUNCAN, G. H., MORALES, F. AND EVANS, A. C. (2002) A general statistical analysis for fMRI data., *NeuroImage*. United States, 15(1), pp. 1–15. doi: 10.1006/nimg.2001.0933.

WORSLEY, K. J., TAYLOR, J. E., TOMAIUOLO, F. AND LERCH, J. (2004) Unified univariate and multivariate random field theory., *NeuroImage*. United States, 23 Suppl 1, pp. S189-95. doi: 10.1016/j.neuroimage.2004.07.026.

YARKONI, T., POLDRACK, R. A., NICHOLS, T. E., VAN ESSEN, D. C. AND WAGER, T. D. (2011) Large-scale automated synthesis of human functional neuroimaging data., *Nature methods*. United States, 8(8), pp. 665–670. doi: 10.1038/nmeth.1635.

ZHAO, J., WANG, J., HUANG, C. AND LIANG, P. (2022) Involvement of the dorsal and ventral attention networks in visual attention span, *Human Brain Mapping*. John Wiley & Sons, Ltd, 43(6), pp. 1941–1954. doi: https://doi.org/10.1002/hbm.25765.